

Analysis of Oxide Scales Formed in the Naphthenic Acid Corrosion of Carbon Steel

Peng Jin,* Gheorghe Bota, Winston Robbins, and Srdjan Nesic

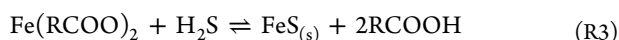
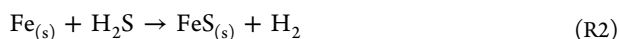
Institute for Corrosion and Multiphase Technology, Ohio University, 342 West State Street, Athens, Ohio 45701, United States

ABSTRACT: Naphthenic acid corrosion of steel is a major challenge in oil refineries. Iron sulfide scales, formed by corrosion due to sulfur compounds found in the crude oil, have shown unpredictable behavior when it comes to their protectiveness. Recent results show that simultaneous formation of an iron oxide scale formed by corrosion due to naphthenic acids may explain part of the variability and contribute to corrosion resistance of the scale formed on 5Cr steel. In depth analysis identified magnetite in the sections of the scale just adjacent to the metal surface. Currently reported research focuses on investigating conditions that lead to the formation of the iron oxide layer on carbon steel. A comparison of different oxide layers formed on carbon steel from a pure model acid (palmitic acid) and a commercial naphthenic acid mixture derived from petroleum shows different behavior when it comes to corrosion protection. The two acids also show different behavior in the presence of sulfur containing compounds (a model compound and native sulfur compounds found in a heavy lube basestock). These results suggest that the molecular structure of the acid is an important factor in the formation and the protectiveness of an iron oxide scale.

1. INTRODUCTION

The carboxylic acid found in petroleum is called “naphthenic acid”.¹ Processing low-price crude oil with high content of naphthenic acid can increase the profit of a medium-size crude oil refinery by over ten million dollars per year.² But naphthenic acid is one of the major causes of high temperature (220–400 °C) corrosion in refinery distillation towers. Naphthenic acid corrosion (NAC) of steel is widely attributed to the formation of soluble iron naphthenates, leaving the steel surface exposed to further attack.³ In contrast, reactive sulfur compounds corrode the steel in the same temperature range (sulfidation) and form insoluble iron sulfide scales.^{4–6} The iron sulfide scales have been researched extensively in the past, given that they have been thought to lead to a decrease in corrosion rates. Because NAC and sulfidation inevitably occur simultaneously, chemical/corrosion engineers face a major challenge in predicting and mitigating high temperature corrosion. Specifically, protective effects of scales have proven to be difficult to predict, not only because of the wide diversity of sulfur compounds found in crude oil but also because of their interaction with naphthenic acids.

The corrosion process is often described by three generic free radical reactions that occur at high temperatures, in the absence of water:



Reaction R1 indicates that naphthenic acids oxidize iron to form oil soluble salts (iron naphthenates) and hydrogen gas. In this reaction, R represents the hydrocarbon portion of the naphthenic acid molecule and COOH is the corrosive carboxylic acid functional group. The reverse reaction is ignored here as it is assumed that there is no buildup of iron naphthenate and hydrogen concentration in the oil.

Some sulfur compounds found in petroleum may react directly with a steel surface, or may first decompose to form hydrogen sulfide, which then reacts with the iron in the steel, as shown by reaction R2, a process often referred to as simply “sulfidation”. In either case insoluble iron sulfide is formed, which remains as a deposit on the steel surface in the form of a scale. Again it is assumed that there is no buildup of hydrogen concentration in the oil and therefore the reverse reaction can be ignored.

A possible interaction between the two corrosion pathways (NAC and sulfidation) is indicated by reaction R3. It is suggested that hydrogen sulfide may react rapidly with the iron naphthenate in the oil phase to form insoluble iron sulfide and “regenerate” the naphthenic acid. Alternatively, in solutions with high concentrations of naphthenic acids the reverse reaction will dominate and the iron sulfide scale may be redissolved. This last possibility leads to a concern that in the presence of naphthenic acids, any protectiveness offered by the iron sulfide scale may be compromised leading to elevated corrosion rates.

The reaction kinetics are dependent on characteristics of the various naphthenic acids and sulfur compounds involved in the process. Crude oil is one of the most complex fluids found in nature, due to the wide variability in its geochemical origin; within any given crude oil sample more than 10⁵ individual components are routinely detected.⁷ Therefore, the naphthenic acids and sulfur compounds present in the crude oil vary widely.

Nowadays, the number of different naphthenic acids identified in heavy crude oils has grown far beyond 3000, detected 15 years ago (where it was assumed that R = C_xH_y, see reaction R1).⁸ It is now recognized that there may be many

Received: May 3, 2016

Revised: June 9, 2016



Table 1. Chemical Composition of A106 Carbon Steel Specimen (wt %)

C	Si	Mn	P	S	Cr	Ni	Mo	V	Cu	Fe
0.18	0.41	0.8	0.11	0.06	0.02	0.04	0.02	0.03	0.08	bal

heteroatom acids present as well (where $R = C_xH_yN_zS_v$).^{9–11} Even more different organo-sulfur compositions can be found in crude oils. Organo-sulfur compositions include nonreactive sulfur compounds (predominantly thiophenes) and reactive sulfur compounds with different molecular structure, functionality and reactivity, such as mercaptans (R–SH), aliphatic and alicyclic sulfides (R–S–R), and disulfides (R–S–S–R).^{12,13}

Given the complexity of crude oils, it is not surprising that it is difficult to correlate any given crude oil composition with the observed corrosion attack. For practical purposes, studies of sulfidation and NAC were frequently related to the total sulfur content (%S) and the total naphthenic acid concentration, as seen in refinery streams, irrespective of the variability in their molecular structure. The %S is routinely determined by X-ray fluorescence (XRF) or other comparable methods. The naphthenic acid concentration is most commonly expressed as the total acid number (TAN), which represents the amount of KOH in milligrams needed to neutralize the naphthenic acid present in one gram of oil, obtained usually by titration.

Sulfidation and NAC studies are difficult as it is hard to reproduce the real conditions encountered in refinery operations in laboratory experiments. High temperature, high velocity, high oil volume/metal area ratio, large time scale of corrosion effects such as growth of corrosion product scales, varying conditions, etc., all make it hard to do convincing laboratory studies. This is probably the reason that the important effect of oil composition has rarely been the focus of previous studies. Few publications deal with the effects of molecular weight and molecular structure of the corrosive species such as naphthenic acids and sulfur compounds.^{14,15} To avoid dealing with the complexity of real crude oils one approach is to work with representative model compounds. This would enable us to investigate the least understood and probably one of the most important factors: the interaction between sulfur compounds and naphthenic acids.

One of the breakthrough discoveries made by the present authors was the identification of a thin protective oxide scale under the much thicker sulfide scale.¹³ Although oxygen in the corrosion product scale had been detected previously in studies of other groups, its presence was dismissed as the exposure to air contamination during or after the experiment.¹⁷ Previously, we reported that naphthenic acids were the source of oxygen in the formation of a protective oxide scale on the surface of chromium steel using a unique experiment protocol. In this protocol, a commercial mixture of naphthenic acids and a model sulfur compound were used to “pretreat” steel specimens in the form of rings to develop a scale and then the scale was attacked by a “challenge” solution containing an elevated concentration of naphthenic acids dissolved in a white mineral oil. This work led to the discovery of a thin oxide scale adjacent to the steel surface that appeared to contribute to the protectiveness against corrosion. This protective oxide scale, characterized as magnetite, has been proposed to arise from thermal decomposition of the iron naphthenate on 5Cr steel surfaces.¹⁶ Other sources of oxygen such as air and water were eliminated as possibilities, as described below.

While the results relating to 5Cr steel have been reported elsewhere,^{16,38} current research focuses on experiments

involving carbon steel. In addition to the native naphthenic acids mixture used previously, this study compares it with the effect produced by a model fatty acid—palmitic acid. The effect of sulfur compound was previously studied by using a model compound: *n*-dodecyl sulfide (DDS) dissolved in white oil, whereas here it was compared with the attack caused by native sulfur compounds found in a Group I lube basestock (yellow oil).

2. EXPERIMENTAL SECTION

2.1. Experiment Materials. Rings made from A106 carbon steel (CS), 81.76 mm outer diameter, 70.43 mm inner diameter, and 5 mm thickness, were used as experiment specimens (for chemical composition of the steel see Table 1). Prior to the experiment, each specimen was polished with 400 and 600-grit silicon-carbide paper (SiC) under the flow of isopropanol in order to avoid oxidation and overheating. Then, the specimen was rinsed with toluene and acetone to clean the surface from any organic deposits and dried under the flow of nitrogen. The weight of the specimen was taken using an analytical balance with the accuracy of 0.1 mg. All experiments were performed by exposing three CS specimens to the corrosive hydrocarbon solution. Two specimens were used for weight loss measurements, and the third was used for microscopic examination.

After the experiment, specimens for weight loss measurements were rinsed with toluene and acetone, dried, brushed to mechanically remove loose scale, exposed to the Clarke solution (ASTM G1-03),^{18,19} to dissolve the remaining scale, dried again, and finally reweighed. The corrosion rate was calculated on the basis of the weight loss, i.e., by subtracting the weight before and after the experiment. Specimens that were examined by microscopy were not subjected to the same cleaning procedure; rather, they were stored in a mineral oil to prevent degradation of the surface scale until time came for analysis, rinsed with toluene and acetone, dried, mounted, and examined using a microscope.

The corrosion product scale formed on specimen surfaces was analyzed by a JEOL JSM-6390 scanning electron microscope (SEM). Some scales were analyzed by FEI Helios Nanolab 650 for focused ion beam (FIB) and Zeiss Libra 200EF transmission electron microscope (TEM). The crystal structure of scale was investigated by X-ray diffraction (XRD) on Bruker Discover D8 with a Co $K\alpha$ X-ray tube.

2.2. Experiment Solutions. Recrystallized *n*-dodecyl sulfide (DDS) by Fisher Chemical was used as a model compound to represent the reactive sulfur compounds found in the crude oil. The mixture of naphthenic acids (TCI) by TCI America (Table 2) was

Table 2. Boiling Point Range of the Model Naphthenic Acid TCI (TAN 230)

parameter	temperature (°C)
initial boiling point (IBP)	239
50% boiling point	296
80% boiling point	343
final boiling point (FBP)	493

used as a model compound for naphthenic acids found in crude oil. Palmitic acid (PA) by Fisher Chemical, which is a simple fatty acid $CH_3(CH_2)_{14}COOH$ with carbon number close to the TCI, was also used as a model acid compound.⁷ These acids and/or DDS were dissolved into a paraffinic white oil solvent (Tufflo 6056, CITGO) in order to prepare the corrosive solutions (see Table 3 for properties of this solvent). In different experiments, acids were dissolved in a “yellow oil” solvent, which is a Group I lube basestock (America’s

Table 3. Selected Physical and Chemical Properties of Model Oil—Tufflo 6056

parameter	description
appearance	clear liquid
color	colorless
odor	odorless
density (at 16 °C, kg/m ³)	876
flash point (°C)	254
average molecular weight (g/mol)	530
initial boiling point (°C)	388

Core 600, Exxon Chemical) with no naphthenic acid and 0.25%S by weight (see Table 4 for its properties).

Table 4. Selected Physical and Chemical Properties of Model Oil—Yellow Oil (America's Core 600)

parameter	description
appearance	clear liquid
color	yellow
odor	odorless
density (at 15 °C, kg/m ³)	879
flash point (°C)	270

There were a few different types of corrosive solutions used in the experiments, which were prepared as follows:

- (1) PA only solution that had no sulfur compounds with only palmitic acid dissolved in Tufflo.
- (2) TCI only solution that had no sulfur compounds with only TCI dissolved in Tufflo.
- (3) PA + DDS solution that had both acidic and sulfur compound obtained by dissolving PA and DDS in Tufflo.
- (4) "TCI + DDS" solution that had both naphthenic acids and sulfur compound obtained by dissolving TCI and DDS in Tufflo.
- (5) PA + Yellow oil solution that had both acidic and sulfur compounds obtained by dissolving PA in Yellow oil.
- (6) "TCI + Yellow oil" solution that had both naphthenic acids and sulfur compounds obtained by dissolving TCI in Yellow oil.
- (7) "Challenge solution" that had no sulfur compounds with only TCI dissolved in Tufflo.

The TAN value and sulfur content of each corrosive solution are shown in Table 5.

Table 5. Properties of Corrosive Solutions

solution	TAN	%S
PA only	0.5, 1, or 1.75	0
TCI only	1.75	0
PA + DDS	1.75	0.25 wt %
TCI + DDS	1.75	0.25 wt %
PA + Yellow oil	1.75	0.25 wt %
TCI + Yellow oil	1.75	0.25 wt %
challenge solution	3.5	0

2.3. Experimental Equipment. The equipment described in our previous publications was used in the present corrosion experiments following the pretreatment/corrosion challenge protocol. A 1 L stirred autoclave was used for the pretreatment of CS specimens. The corrosion challenge was performed in a so-called high velocity rig (HVR) which is a flow-through rotating cylinder reactor. As depicted in our prior publication, the HVR was designed to create a high flow velocity and associated turbulence and shear stress.²⁰ The CS specimens were mounted on a mandrel in the core of the HVR

reactor and rotated. The cross section of the HVR reactor is shown in Figure 1.

2.4. Experimental Protocol. The pretreatment/corrosion challenge experiment protocol consisted of two consecutive steps:

- the *pretreatment* step used to create the corrosion product scale in different solutions as listed in Table 5 and
- the *corrosion challenge* step where the scale was exposed to the challenge solution.

For the pretreatment in the stirred autoclave, the corrosion product scale formed on specimens that were fully immersed in 0.7 L corrosive solution. Before the starting of the pretreatment, the headspace of autoclave was purged with nitrogen gas to remove oxygen. During a 24 h pretreatment at 343 °C, the specimens were stagnant while mixing was done by an impeller rotating at 500 rpm. At the end of the pretreatment, the autoclave was cooled and the oil was drained, the specimens rinsed, and used for weight loss and microscopic analysis. Another parallel pretreatment experiment was run under same conditions, but specimens with their intact corrosion product scales were transferred to the HVR for the challenge step.

In the corrosion challenge, pretreated specimens were mounted in the HVR, heated to 343 °C as hot Tufflo flowed through the reactor. The specimens were rotated at 2000 rpm (corresponding to a peripheral velocity of 8.56 m/s, Reynolds number of 1771, and wall shear stress of 74 Pa). The actual corrosion challenge experiment began when the input flow was switched from Tufflo to the challenge solution, and lasted for 24 h with the challenge solution flowing through the reactor at 7.5 cm³/min. The back-pressure of 150 psig was applied to suppress gas breakout. The corrosion challenge ended when the flow was switched back to Tufflo. The specimens were allowed to cool in Tufflo before being removed from the HVR for analysis.

2.5. Evaluation of Corrosion Rates. Time averaged corrosion rates of the specimens were calculated based on their weight loss during the experiment. For the pretreatment experiment conducted in the stirred autoclave, the corrosion rate was calculated as follows:

$$CR_{\text{pretreatment}} = \frac{(IW - FW)}{\rho_{\text{steel}} A_s \text{pretreatment} t_{\text{pretreatment}}} \times 10 \times 24 \times 36 \quad (1)$$

where $CR_{\text{pretreatment}}$ is pretreatment corrosion rate [mm/y]; IW is initial weight of freshly polished specimen [g], FW is final weight of specimen after treatment with Clarke solution [g], ρ_{steel} is density of specimen [g/cm³], $A_s \text{pretreatment}$ is area of specimen exposed to corrosive fluid during pretreatment [cm²], $t_{\text{pretreatment}}$ is duration of pretreatment [h].

In the corrosion challenge step, the freshly polished specimen was first pretreated in the autoclave followed by the corrosion challenge in the HVR. The challenge corrosion rate was calculated as follows:

$$CR_{\text{challenge}} = \frac{(IW - FW - WL_{\text{pretreatment}})}{\rho_{\text{steel}} A_s \text{challenge} t_{\text{challenge}}} \times 10 \times 24 \times 36 \quad (2)$$

where $CR_{\text{challenge}}$ is net corrosion rate from the corrosion challenge step (excluding the pretreatment step) [mm/y], IW is initial weight of freshly polished specimen [g], FW is final weight of specimen after treatment with Clarke solution [g], $WL_{\text{pretreatment}}$ is weight loss of specimen in the pretreatment step [g], ρ_{steel} is density of specimen [g/cm³], $A_s \text{challenge}$ is area of specimen exposed to corrosive fluid during challenge [cm²], $t_{\text{challenge}}$ is duration of corrosion challenge [h].

3. RESULTS AND DISCUSSION

3.1. Effect of Palmitic Acid Concentration on Formation of Oxide Scale. Corrosion rates measured for the CS specimens during the pretreatment step at different TAN (PA concentrations) are shown in Table 6. The thickness of the corrosion product scale was proportional to the PA concentration (TAN) as seen in the cross-section SEM images below, Figure 2a–c. The EDS analysis shows that the scale is

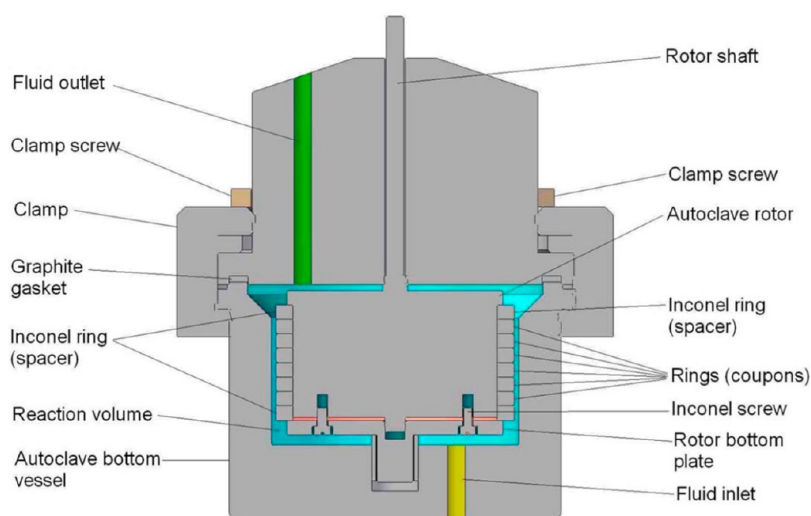


Figure 1. Cross-sectional view of HVR reactor.

Table 6. Pretreatment Corrosion Rates of CS Specimens in the PA Only Solution

TAN of PA only solution	pretreatment corrosion rate (mm/y)
0.5	0.1
1	0.2
1.75	0.2

rich in oxygen (Figure 2a'–c'). The specimen with the thickest scale, exposed to the TAN 1.75 solution, was selected as a baseline for the subsequent experimentation.

3.2. Effect of Sulfur Compounds on Oxide Scale Formed in the Presence of Palmitic Acid. In order to assess the effect of sulfur compounds on the protectiveness of the oxide scale formed in the presence of PA, the CS specimens were pretreated in the autoclave and then challenged in the HVR. As shown in Table 7, solutions at TAN 1.75 were either a PA only solution (used as a baseline), or one of the two sulfur containing solutions: PA + Yellow oil or PA + DDS.

In the pretreatment step, it was found that the corrosion rates of specimens exposed to PA + DDS solution were much higher than those exposed to a PA + Yellow oil, suggesting that DDS is more corrosive than the native sulfur compounds in

Table 7. Pretreatment and Challenge Corrosion Rates of CS Specimens Pretreated in PA only, PA + DDS, and PA + Yellow Oil

pretreatment solution	TAN 1.75 pretreatment corrosion rate (mm/y)	TAN 3.5 challenge corrosion rate (mm/y)
PA only %S = 0 wt %	0.2	4.8
PA + DDS %S = 0.25 wt %	0.7	4.2
PA + Yellow oil %S = 0.25 wt %	0.4	1.8
bare steel TAN 3.5 corrosion rate ^a		7.8

^aFreshly polished specimens (no surface scale) were installed in the HVR and corroded by the challenge solution under corrosion challenge conditions.

Yellow oil. In both cases the corrosion rates were higher than those measured for the PA only solution.

In the TAN 3.5 corrosion challenge step, the scale formed in PA only proved to be least protective, followed by the scale formed in the PA + DDS solution, with the scale formed in the PA + Yellow oil being most protective, as shown in Table 7. To put these corrosion rate numbers into context, the bare steel

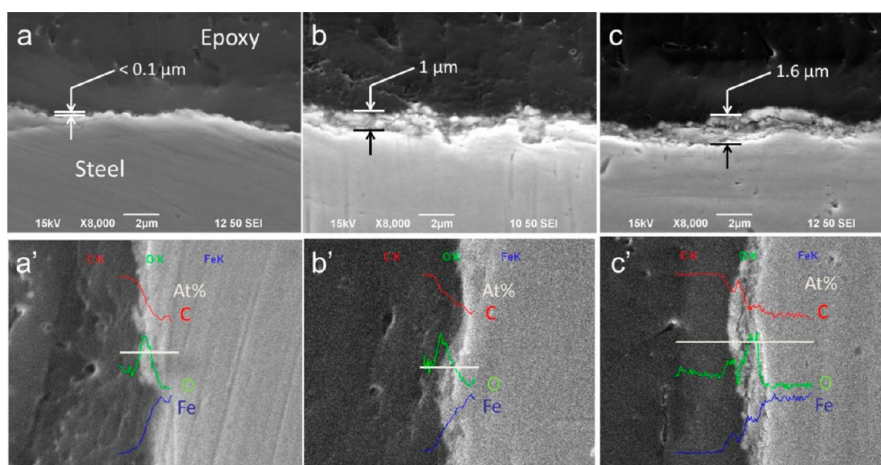


Figure 2. Cross-sectional SEM images of CS specimens pretreated with PA only of TAN 0.5 (a), TAN 1 (b), and TAN 1.75 (c). (a'–c') Results of corresponding EDS analyses performed along the white line.

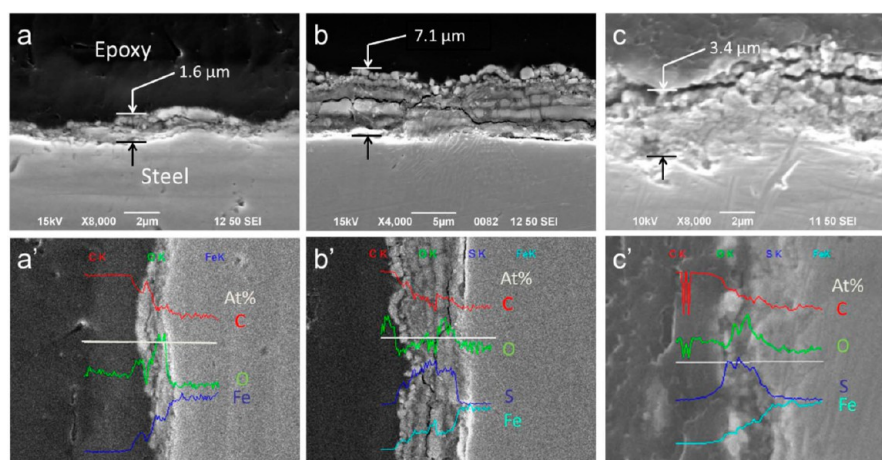


Figure 3. Cross-section SEM images of CS specimens pretreated with (a) PA only, (b) PA + DDS, or (c) PA + Yellow oil. (a'–c') Results of corresponding EDS analysis performed along the white line.

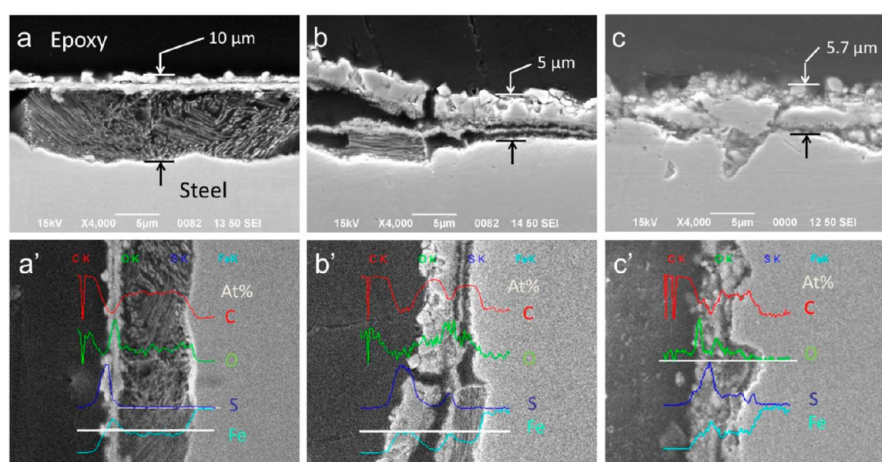


Figure 4. Cross-sectional SEM images of CS rings after pretreatment and TAN 3.5 corrosion challenge: (a) PA only, (b) PA + DDS, and (c) PA + Yellow oil. (a'–c') Results of corresponding EDS analysis performed along the white line.

corrosion rate obtained in a TAN 3.5 corrosion experiment (without sulfur compounds) is also shown there.

The scales formed during the pretreatment step on specimen exposed to the sulfur containing PA + DDS and PA + Yellow oil solutions (shown in Figure 3b and c) are much thicker than that formed in the sulfur-free PA only solution (shown in Figure 3a). With the presence of DDS, the scale is thickest (around 7 μm) and composed of cracked layers that appear to contain predominantly iron and sulfur, as shown by the EDS analysis (Figure 3b). Oxygen is also detected but appears to be distributed within the iron sulfide layers. The scale formed on the specimen in the PA + Yellow oil solution is much thinner (around 3 μm), less granular, and the peak of oxygen appears closer to the steel surface.

The challenge corrosion rates for the pretreated specimens reveal differences in protectiveness among the scales (Table 7). The scale formed in PA only reduces the challenge corrosion rate by about one-third. Although PA + DDS pretreatment generated a thicker scale, the protection appears to be similar to PA only solution. On the other hand, the scale formed in PA + Yellow oil is most protective. The appearance of the different scales remaining on the surface after the corrosion challenge is shown in SEM images in Figure 4.

The scale originally present on specimens pretreated with PA only was almost entirely dissolved, which is consistent with lack of protectiveness (Figure 4a). The lamellar structure seen on the surface is a remnant of a grain of pearlite (solid solution of α -ferrite and cementite Fe_3C , a characteristic of austenitic steel). Note that there is a thin sulfide/oxide layer on the outer surface of the pearlite. Similar thin, outer sulfide and oxide layers have been seen with TCI in HVR parameter studies in the development of the corrosion challenge conditions.²¹ In those studies, nonprotective oxide layers were observed to grow with temperature, time and TCI concentration. Thus, the scales formed in PA only solutions adhere poorly and offer limited resistance to naphthenic acids.

The scale formed in the PA + DDS solution survived the corrosion challenge but shows evidence of delamination as well as undermining which explains the poor protection this scale offered during the corrosion challenge (Figure 4b). On the other hand, the scale formed in PA + Yellow oil remained adherent after the corrosion challenge (Figure 4c). EDS analysis shows oxygen peaks on both sides of a tight sulfide layer.

3.3. Effect of Sulfur Compounds on Oxide Scale Formed in TCI. As a baseline for this series of experiments the pretreatment was done in TCI only solution at TAN 1.75 (see

Table 8). The pretreatment corrosion rate in TCI only solution was slightly higher than that in PA only solution at the same

Table 8. Pretreatment and Challenge Corrosion Rates of CS Specimens Pretreated in TCI Only, TCI + DDS, and TCI + Yellow Oil

pretreatment solution	pretreatment corrosion rate (mm/y)	challenge corrosion rate (mm/y)
TCI only TAN 1.75, %S = 0 wt %	0.5	6.6
TCI + DDS TAN 1.75, %S = 0.25 wt %	0.6	8.6
TCI + Yellow oil TAN 1.75, %S = 0.25 wt %	0.4	1.3
bare steel TAN 3.5 corrosion rate ^a		7.8

^aFreshly polished specimens (no surface scale) were installed in the HVR and corroded by the challenge solution under corrosion challenge conditions.

TAN 1.75 and both pretreatments resulted in challenge corrosion rates comparable with the bare steel TAN 3.5 corrosion rate. When DDS was added to the pretreatment solution (TCI + DDS solution), the challenge corrosion rate was still high. The most protective scale was formed in the TCI + Yellow oil solution.

SEM/EDS analyses of cross-section of scales formed in TCI only, TCI + DDS, and TCI + Yellow oil solutions are shown in Figure 5. In the TCI only solution, a delaminated scale was formed (much thinner than the scale formed in the PA only solution) and EDS analysis suggests that it is composed of iron, sulfur and oxygen with carbon possibly coming from a pearlitic structure. The scale formed in TCI + DDS solution that is much thicker is comprised of successive layers containing oxygen and sulfur closer to the steel surface, covered by outer layer composed mostly of sulfur. While oxygen is found in inner layers, the layer closest to the metal substrate appears to be a sulfide. Despite the presence of oxygen in the scale (Figure 5), neither of the scales adhered as well as that formed by PA + Yellow oil. The scale formed in TCI + Yellow oil is thin and adherent to the steel surface. EDS analysis shows the peak of oxygen adjacent to the steel surface.

The pretreatment in TCI + Yellow oil lowered the challenge corrosion rate, but the TCI + DDS pretreatment had little effect. Both PA and TCI gave similar response in Yellow oil, but they behaved differently with or without DDS in Tufflo. Therefore, following analyses focus on the difference of scales formed in PA and TCI.

3.4. Morphology and Composition of Oxide Scale Formed in Acidic Solutions. SEM analyses show the presence of thin oxide scales on both PA only and TCI only pretreated rings (Figures 2 and 5). The PA scale appears to be $\sim 2 \mu\text{m}$ thick with an outer layer richer in carbon and the inner oxygen layer closer to the metal (Figure 2c). In contrast, the scale formed in TCI only appears to be thicker ($>2 \mu\text{m}$) consisting of both an outer $\sim 1 \mu\text{m}$ sulfur/oxygen layer and an inner $\sim 1 \mu\text{m}$ layer that appears to be pearlitic (Figure 5). However, the SEM resolution is not high enough to reveal the detailed scale morphology. Therefore, segment of scale from each were extracted by FIB and examined by high resolution TEM and EDS.

The image for the PA only pretreatment scale shows a distribution of small ($<100 \text{ nm}$), isolated particles above a thin continuous layer ($\sim 100 \text{ nm}$) adjacent to the steel surface (Figure 6). The thin layer of iron and oxygen is more clearly seen in TEM/EDS mapping of the surface (Figure 7). Atomic O/Fe ratios ($\sim 60/40$) for selected areas are consistent for both the particle and the inner layer. XRD analysis of the surface detects the presence of magnetite and ferrite α -iron (Figure 8).

According to the SEM analysis, the scale formed in TCI only is thicker than the one formed with PA only and appears to show multiple layers (Figure 5). TEM images (Figure 9) and EDS mapping of the TEM area (Figure 10) give clear definition of the composition of these layers. The outer smooth gray layer is composed of iron and oxygen along with sulfur that may be traced to the small concentration of native sulfur in the TCI. Underneath the outer layer, the inner layer is rich in oxygen and deficient in sulfur. The stripped structure in the inner layer appears to have the characteristic banding of pearlite. Further, the EDS mapping shows that the light stripes are enriched in Fe but deficit in O, suggesting that they are cementite (Fe_3C). On the other hand, the darker area between the stripes (area B, for example) is oxygen rich, suggesting oxidation of ferrite within the pearlite grain. The O/Fe ratio (60:40) for the grain interior appears similar to that for the tight layer in the PA case. Closer

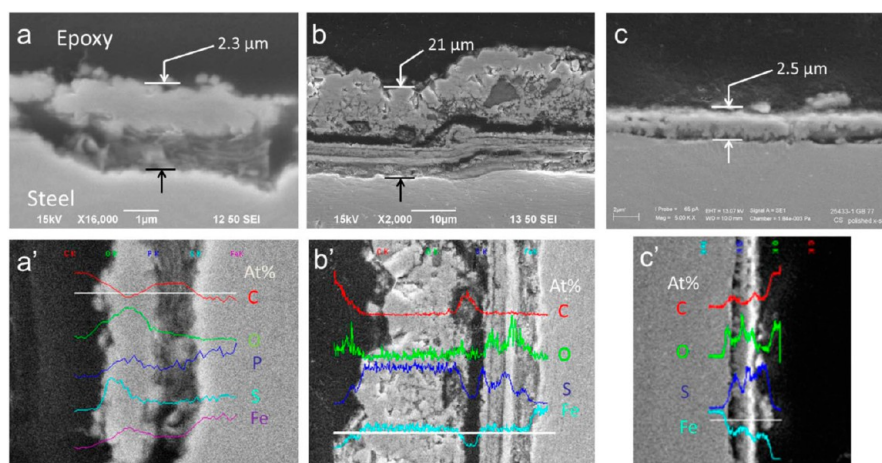
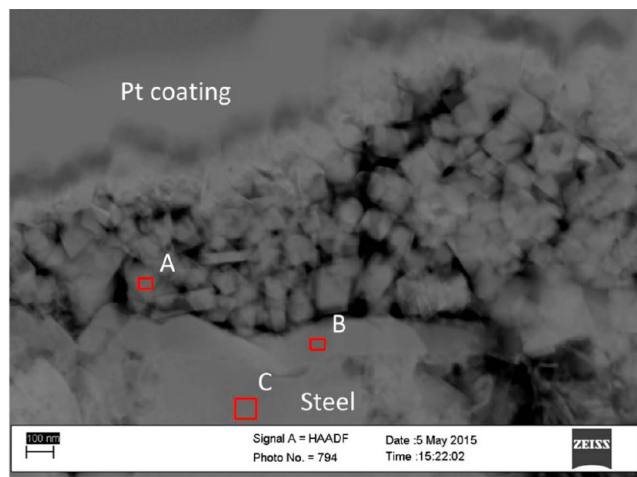


Figure 5. Cross-section SEM images of CS specimens pretreated with TCI only solution (a), TCI + DDS solution (b), and TCI + Yellow oil solution. (a'–c') Results of corresponding EDS analysis performed along the white line.



A		B		C	
Element	Atomic%	Element	Atomic%	Element	Atomic%
C	0	C	0	C	0
O	53.8	O	60.2	O	0
S	0.1	S	0	S	0
Fe	46.1	Fe	39.8	Fe	100.0

Figure 6. TEM image and EDS analysis of the scale formed on the CS specimen pretreated in PA only solution. EDS analysis was performed in three square areas.

to the metal surface, the O/Fe ratio decreases and some voids appear at the interface between the grain and the steel surface, i.e. the layer under the pearlite is discontinuous. These voids appear to be at the end of some of the iron oxide bands in grain. Neither of the two scales formed in acidic solutions were protective in the corrosion challenge, which could be possibly

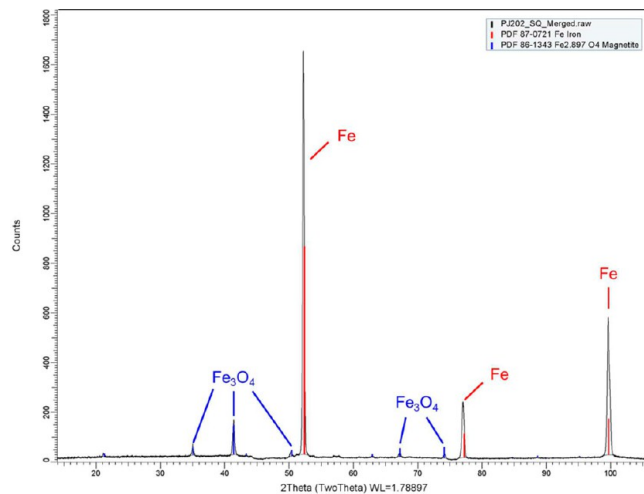


Figure 8. XRD analysis on the bulk CS specimen pretreated in PA only solution.

related to the poor adherence of these scales to the steel surface.

3.5. Discussion on the Formation Mechanism of Oxide Scale in Acidic Solutions. NAC was generally considered to generate no solid corrosion product on the steel surface, although the formation of oxide scale has been noted in the literature. For instance, El Kamel and co-workers found the presence of an iron oxide scale on the specimen corroded by a crude fraction in the autoclave.¹⁷ In another study it was reported that the corrosion by a crude oil containing high content of naphthenic acids left a layer of magnetite.²² Huang found magnetite after the corrosion by a model naphthenic acid.²³ However, these observations were

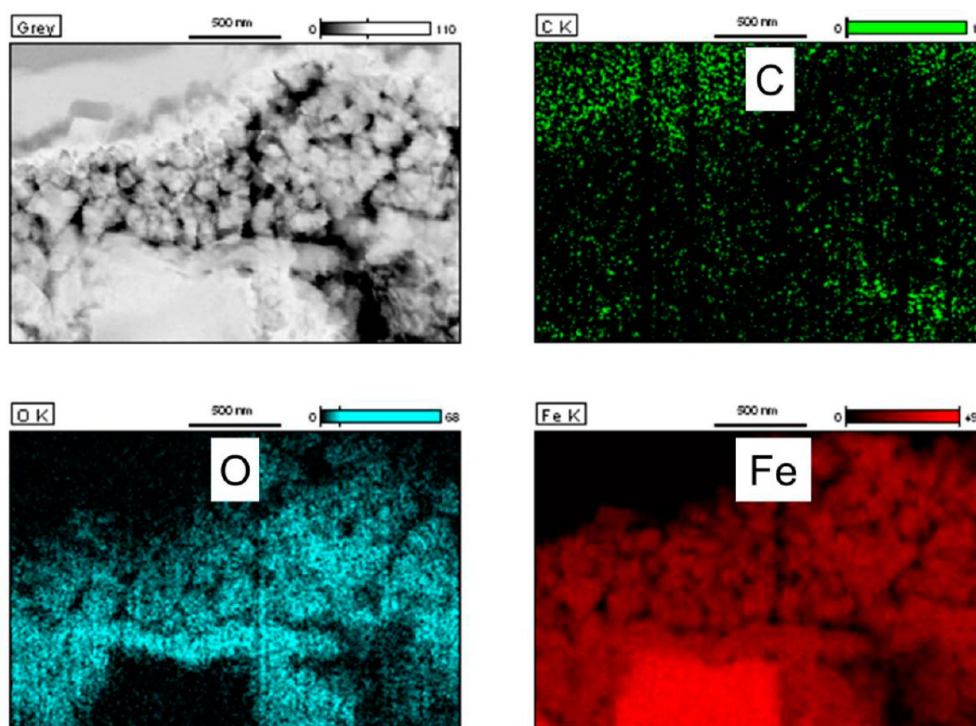
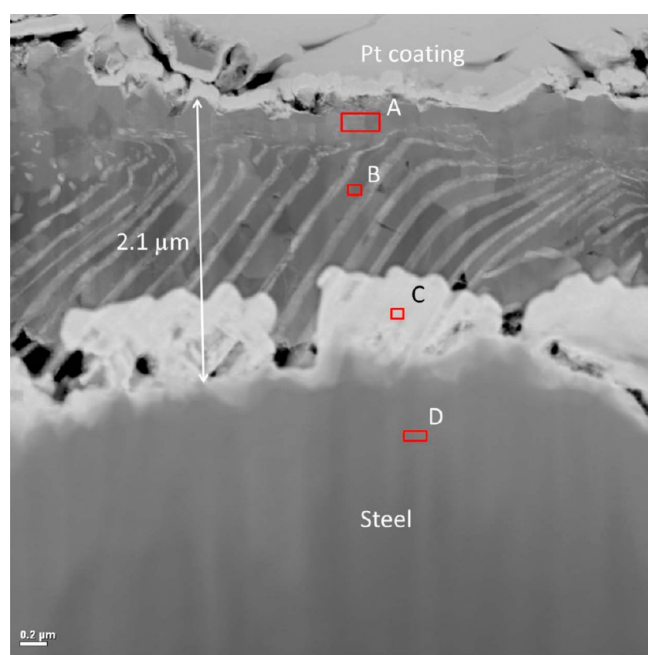


Figure 7. EDS mapping of the scale formed on the CS specimen pretreated in PA only solution.



A		B		C		D	
Element	Atomic%	Element	Atomic%	Element	Atomic%	Element	Atomic%
O	45.8	O	61.9	O	36.8	O	1.6
S	13.3	S	0.1	S	1.3	S	0.2
Fe	40.8	Fe	37.9	Fe	61.8	Fe	98.3

Figure 9. TEM image and EDS analysis of the scale formed on the CS specimen pretreated in TCI only solution. EDS analysis was performed in four square areas.

dismissed and considered as contamination of the sample or the artifact of the experiment.

In our prior research, specimens were pretreated by a mixture of natural naphthenic acids dissolved in the mineral oil following the same pretreatment procedure in sections above. A protective oxide scale composed of magnetite was found on the surface. The pretreatment in the solution containing both TCI and DDS resulted in an oxide scale adjacent to the steel surface an iron sulfide scale on the outside.¹⁶ After the pretreatment at low temperature (232 °C), no oxide scale was formed even in the presence of naphthenic acids.²⁴ These findings have explicitly proven that the oxide scale was not formed due to the specimen oxidation before nor oxidation of iron sulfide scale after the experiment, and therefore was neither due to contamination nor was it an artifact.

The positive correlation between the TAN and the oxide scale thickness found in the present study (see Figure 2) clearly indicates that the oxide scale was formed during the pretreatment at high temperatures. The source of oxygen was postulated to be naphthenic acids, the only oxygen-containing compound in the experimental solution.

In order to further confirm the source of oxygen found in the oxide scale, specimens were pretreated in Tufflo (containing no naphthenic acids or any sulfur compounds). The specimen was not corroded and no oxygen was detected in the EDS analysis as was formed in the presence of naphthenic acids.

Therefore, it has been confirmed that the oxide scale was formed during the NAC. Deeper literature review suggested that the oxide scale may be formed due to the thermal decomposition of iron naphthenates as shown by reactions R4 and R5 below. Reaction R4 belongs to ketonization which has been utilized for over 150 years to prepare ketone (RCOR) via the decomposition of metal carboxylate at elevated temperatures (300 to 400 °C).^{25–27} Historically, organic acids were heated with iron powder to form solid iron carboxylates at

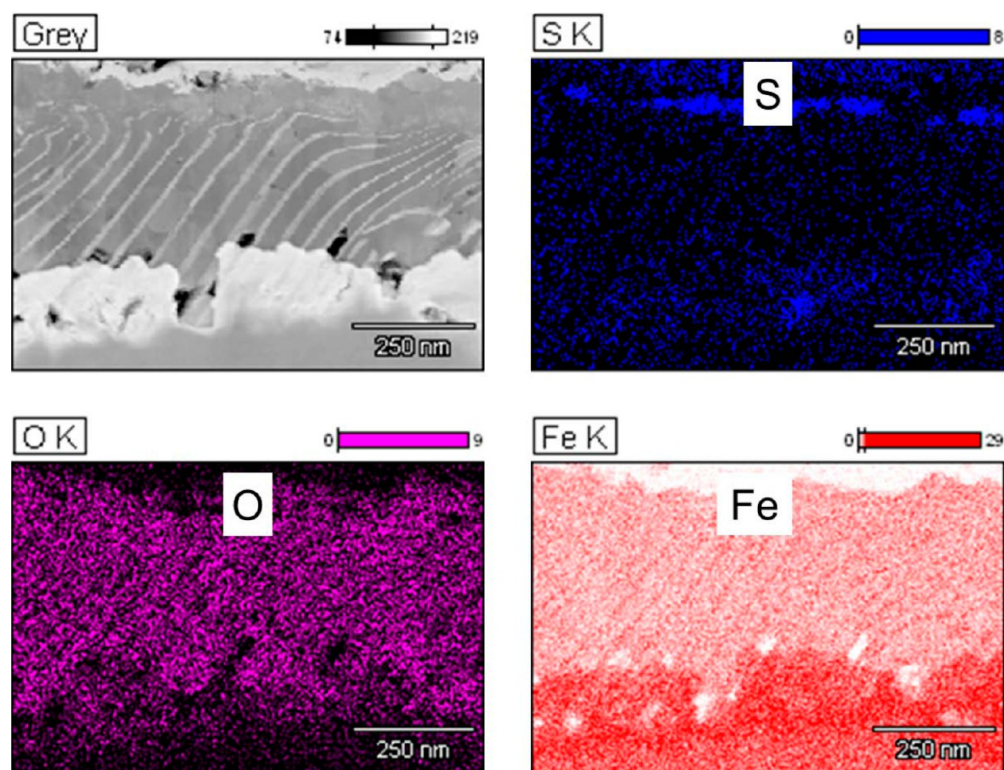
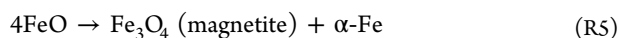
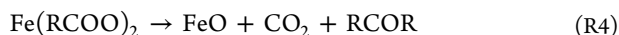


Figure 10. EDS mapping of the scale formed on the CS specimen pretreated in TCI only solution.

temperatures around 200 °C that were subsequently pyrolyzed at temperatures higher than 275 °C to form ketones in high yields.²⁸ In recent decades, the ketonization of iron carboxylates received increasing attention in the formation of nano-particulate magnetite (Fe₃O₄) which embraced a wide range of applications, including electronic data storage and catalysis.^{28–31} In-depth investigation on the reaction mechanism suggested that initially formed wüstite (FeO) is thermally unstable below 500 °C and disproportionates to form magnetite (reaction R5).^{32,33}



Products of reactions R4 and R5 were also reported in prior studies of NAC. Magnetite was found as the product of thermal decomposition of iron naphthenates between 200 and 800 °C.³⁴ Short-term exposure of sample solutions to excess iron powder at series of temperatures has been used to characterize the reactivity of different oils.³⁵ Application of this technique to model fatty acids noted that the corrosion rates continued to rise with temperature, but iron concentration in solution decreased above 260 °C while more carbon dioxide (CO₂) was generated at higher temperatures.³⁶ The literature also suggested that iron carboxylates decomposition in hydrocarbon solution was complete within an hour at about 300 °C, i.e., ketonization can occur within the time frame of the corrosion experiment.²⁸ Recently, the ketone generated in reaction R4 was found to correlate with the amount of iron corroded in NAC.³⁷ However, none of these studies mentioned the formation of the magnetite scale in the corrosion or addressed the role of the steel surface and scale during sulfidation and NAC.

On the basis of the literature as well as current results, the formation of the oxide scale is hypothesized as follows. First, NAC occurs at the steel surface. The naphthenic acid has to diffuse outward and the corresponding iron naphthenate has to desorb from the iron and diffuse back to the bulk fluid. Because the iron naphthenate has twice size of the acid alone, its diffusion is much slower, keeping it on the surface longer. Under the sulfide scale, faster decomposition of the iron naphthenate allows it to form wüstite while additional acid diffuses through the scale toward the steel surface. The wüstite is thermodynamically unstable and can disproportionate to magnetite and α -iron. The latter is available to react with naphthenic acids but it appears that some iron-rich particles survive adjacent to the steel surface (Figure 9). Because it is oxidized, the iron in magnetite is resistant to acid dissolution. If the formation rate of wüstite (and hence magnetite) exceeds the rate of NAC, a continuous scale of magnetite adjacent to the steel surface can be formed.

The different behavior of TCI and PA in the presence of the sulfur compounds is hypothesized to be related to the relative corrosion rates of NAC and sulfidation. If the sulfidation kinetics are faster than those of NAC as the case with DDS, then sulfidation interrupts the formation of a continuous magnetite layer, resulting in discrete magnetite particles. On the other hand, if the NAC kinetics are faster than the sulfidation, then the oxide layer can be formed providing a diffusion barrier to the steel surface. In this later case, lower corrosion rate continues with iron sulfide formed as an outer scale by the reaction of iron naphthenate. Work is ongoing in this laboratory to more clearly characterize the role of the surface

morphology on oxide formation, to determine the effect of acid structure on the protection, and to elucidate the role of the classes and structures of the sulfur compounds responsible for the different kinetics.

4. CONCLUSION

The thin oxide scale (thickness in nanometers) was formed during the corrosion by a mixture of naphthenic acids or a pure acid. The acid structure was an important factor in the morphology of the oxide scale. It suggested that the tendency to form the oxide scale was not uniform among naphthenic acids. Moreover, the role of sulfur compounds in protectiveness of the scale cannot be neglected. Reactive model sulfur compounds, DDS for example, interrupted the formation of the oxide scale and compromised its protectiveness. Other sulfur compounds, including those natural occurring in Yellow oil, enhance the scale protectiveness. Further research will focus on the role of different naphthenic acids and sulfur compounds on the formation of scale and its protectiveness.

■ AUTHOR INFORMATION

Corresponding Author

*E-mail: pj221108@ohio.edu. Tel.: +1-740-593-0283. Fax: +1-740-593-9949 (P.J.).

Notes

The authors declare no competing financial interest.

■ ACKNOWLEDGMENTS

This work was supported by Naphthenic Acid Corrosion Joint Industry Project (NAP JIP) in the Institute for Corrosion and Multiphase Technology, Ohio University.

■ ABBREVIATIONS

NAC = naphthenic acid corrosion

DDS = *n*-dodecyl sulfide

PA = palmitic acid

TCI = mixture of naphthenic acids available from TCI America

CS = carbon steel

■ REFERENCES

- (1) Derungs, W. A. Naphthenic Acid Corrosion—An Old Enemy of the Petroleum Industry. *Corrosion* **1956**, *12*, 41–46.
- (2) Kapusta, S. D.; Ooms, A.; Smith, A.; Fort, W. C. Safe Processing of Acid Crudes. *CORROSION/2004*, New Orleans, LA, March 28–April 1, 2004; Paper No. 4637.
- (3) Slavcheva, E.; Shone, B.; Turnbull, A. Review of Naphthenic Acid Corrosion in Oil Refining. *Br. Corros. J.* **1999**, *34*, 125–131.
- (4) Couper, A. S. High Temperature Mercaptan Corrosion of Steels. *Corrosion* **1963**, *19*, 396–401.
- (5) Jin, P.; Farelis, F.; Robbins, W.; Bota, G.; Nestic, S. Generation of H₂S by Crude Fractions at High Temperature. In *Abstr. Pap. Am. Chem. Soc.*; American Chemical Society: Washington, DC, 2014; Vol. 248, pp 544–545.
- (6) Jin, P. Mechanism of Corrosion by Naphthenic Acids and Organosulfur Compounds at High Temperatures. Ph.D. Dissertation, Ohio University, Athens, Ohio, USA, 2013.
- (7) Hsu, C.; Dechert, G.; Robbins, W.; Fukuda, E. Naphthenic Acids in Crude Oils Characterized by Mass Spectrometry. *Energy Fuels* **2000**, *14*, 217–223.
- (8) Qian, K.; Robbins, W.; Hughey, C.; Cooper, H.; Rodgers, R.; Marshall, A. Resolution and Identification of Elemental Compositions for More Than 3000 Crude Acids in Heavy Petroleum by Negative-ion

Microelectrospray High-field Fourier Transform Ion Cyclotron Resonance Mass Spectrometry. *Energy Fuels* **2001**, *15*, 1505–1511.

(9) Headley, J. V.; McMartin, D. W. A Review of the Occurrence and Fate of Naphthenic Acids in Aquatic Environments. *J. Environ. Sci. Health, Part A: Toxic/Hazard. Subst. Environ. Eng.* **2004**, *39*, 1989–2010.

(10) Tomczyk, N. A.; Winans, R. E.; Shinn, J. H.; Robinson, R. C. On the Nature and Origin of Acidic Species in Petroleum. 1. Detailed Acid Type Distribution in a California Crude Oil. *Energy Fuels* **2001**, *15*, 1498–1504.

(11) Hughey, C. A.; Rodgers, R. P.; Marshall, A. G.; Qian, K.; Robbins, W. K. Identification of Acidic NSO Compounds in Crude Oils of Different Geochemical Origins by Negative Ion Electrospray Fourier Transform Ion Cyclotron Resonance Mass Spectrometry. *Org. Geochem.* **2002**, *33*, 743–759.

(12) Liu, P.; Shi, Q.; Chung, K. H.; Zhang, Y.; Pan, N.; Zhao, S.; Xu, C. Molecular Characterization of Sulfur Compounds in Venezuela Crude Oil and Its SARA Fractions by Electrospray Ionization Fourier Transform Ion Cyclotron Resonance Mass Spectrometry. *Energy Fuels* **2010**, *24*, 5089–5096.

(13) Lobodin, V. V.; Robbins, W. K.; Lu, J.; Rodgers, R. P. Separation and Characterization of Reactive and Non-Reactive Sulfur in Petroleum and Its Fractions. *Energy Fuels* **2015**, *29*, 6177–6186.

(14) Dettman, H. D.; Li, N.; Wickramasinghe, D.; Luo, J. The Influence of Naphthenic Acid and Sulphur Compound Structure on Global Crude Corrosivity under Vacuum Distillation Conditions. *NACE 2010 Northern Area Western Conference*, Calgary, Alberta, Canada, February 15–18, 2010.

(15) Turnbull, A.; Slavcheva, E.; Shone, B. Factors Controlling Naphthenic Acid Corrosion. *Corrosion* **1998**, *54*, 922–930.

(16) Jin, P.; Nestic, S.; Wolf, H. A. Analysis of Corrosion Scales Formed on Steel at High Temperatures in Hydrocarbons Containing Model Naphthenic Acids and Sulfur Compounds. *Surf. Interface Anal.* **2015**, *47*, 454–465.

(17) El Kamel, M.; Galtayries, A.; Vermaut, P.; Albinet, B.; Foulonneau, G.; Roumeau, X.; Roncin, B.; Marcus, P. Sulfidation Kinetics of Industrial Steels in a Refinery Crude Oil at 300 C: Reactivity at the Nanometer Scale. *Surf. Interface Anal.* **2010**, *42*, 605–609.

(18) *Annual Book of ASTM Standards*; ASTM: West Conshohocken, PA, 2011; Vol. 03.02.

(19) Clarke, S. G. The Use of Inhibitors (with Special Reference to Antimony) in the Selective Removal of Metallic Coatings and Rust. *Trans. Electrochem. Soc.* **1936**, *69*, 131–144.

(20) Bota, G. M.; Qu, D.; Nestic, S.; Wolf, H. A. Naphthenic Acid Corrosion of Mild Steel in the Presence of Sulfide Scales Formed in Crude Oil Fractions at High Temperature. *CORROSION/2010*, San Antonio, Texas, USA, March 14–18, 2004; Paper No. 10353.

(21) Bota, G. M.; Corrosion of Steel at High Temperature in Naphthenic Acid and Sulfur Containing Crude Oil Fractions. PhD dissertation, Ohio University, Athens, OH, 2010.

(22) Smart, N. R.; Rance, A. P.; Pritchard, A. M. Laboratory Investigation of Naphthenic Acid Corrosion Under Flowing Conditions. *CORROSION/2002*, Denver, Colorado, USA, April 7–11, 2002; Paper No. 02484.

(23) Huang, B. S.; Yin, W. F.; Sang, D. H.; Jiang, Z. Y. Synergy Effect of Naphthenic Acid Corrosion and Sulfur Corrosion in Crude Oil Distillation Unit. *Appl. Surf. Sci.* **2012**, *259*, 664–670.

(24) Jin, P.; Robbins, W.; Bota, G.; Nestic, S. Characterization of Iron Oxide Scale Formed in Naphthenic Acid Corrosion. In *Characterization of Minerals, Metals, and Materials 2016*; Ikhmayies, S. J., Li, B., Carpenter, J. S., Hwang, J. Y., Monteiro, S. N., Li, J., Firrao, D., Zhang, M., Peng, Z., Escobedo-Diaz, J. P., Bai, C., Eds.; John Wiley & Sons, Inc.: Hoboken, NJ, 2016; pp 117–125.

(25) Friedel, C. Ueber s. g. gemischte Acetone. *Justus Liebigs Annalen der Chemie* **1858**, *108*, 122–125.

(26) Squibb, E. R. Improvement in the Manufacture of Acetone. *J. Am. Chem. Soc.* **1895**, *17*, 187–201.

(27) Renz, M. Ketonization of Carboxylic Acids by Decarboxylation: Mechanism and Scope. *Eur. J. Org. Chem.* **2005**, *6*, 979–988.

(28) Hadebe, S. W.; Leckel, D. Iron Removal from High-Temperature Fischer–Tropsch-Derived Distillate through Thermal Treatment. *Energy Fuels* **2013**, *27*, 5161–5167.

(29) Baaziz, W.; Pichon, B. P.; Fleutot, S.; Liu, Y.; Lefevre, C.; Greneche, J. M.; Toumi, M.; Mhiri, T.; Begin-Colin, S. Magnetic Iron Oxide Nanoparticles: Reproducible Tuning of the Size and Nanosized-dependent Composition, Defects, and Spin Canting. *J. Phys. Chem. C* **2014**, *118*, 3795–3810.

(30) Redl, F. X.; Black, C. T.; Papaefthymiou, G. C.; Sandstrom, R. L.; Yin, M.; Zeng, H.; Murray, C. B.; O'Brien, S. P. Magnetic, Electronic, and Structural Characterization of Nonstoichiometric Iron Oxides at the Nanoscale. *J. Am. Chem. Soc.* **2004**, *126*, 14583–14599.

(31) Chen, C. J.; Lai, H. Y.; Lin, C. C.; Wang, J. S.; Chiang, R. K. Preparation of Monodisperse Iron Oxide Nanoparticles via the Synthesis and Decomposition of Iron Fatty Acid Complexes. *Nanoscale Res. Lett.* **2009**, *4*, 1343–1350.

(32) Stolen, S.; Gloeckner, R.; Gronvold, F. Nearly Stoichiometric Iron Monoxide Formed as a Metastable Intermediate in a Two-Stage Disproportionation of Quenched Wüstite. Thermodynamic and Kinetic Aspects. *Thermochim. Acta* **1995**, *256*, 91–106.

(33) Hermankova, P.; Hermanek, M.; Zboril, R. Thermal Decomposition of Ferric Oxalate Tetrahydrate in Oxidative and Inert Atmospheres: the Role of Ferrous Oxalate as an Intermediate. *Eur. J. Inorg. Chem.* **2010**, *7*, 1110–1118.

(34) Fukushima, J.; Kodaira, K.; Matsushita, T. J. Preparation and Formation Process of Various Iron Oxide Films by Thermal Decomposition of Iron Naphthenate. *Yogyo Kyokaiishi* **1976**, *84*, 529–533.

(35) Lorenzo, R.; Hau, J. L.; Yepez, O.; Specht, M. I. The Iron Powder Test for Naphthenic Acid Corrosion Studies. *CORROSION/99*, San Antonio, Texas, USA, April 25–30, 1999; Paper No. 99379.

(36) Yépez, O. On the Chemical Reaction between Carboxylic Acids And Iron, Including the Special Case of Naphthenic Acid. *Fuel* **2007**, *86*, 1162–1168.

(37) Barney, M. M.; Miao, T. Z.; Cheng, M. T. H.; Kusinski, G. J. Methods for Evaluating Corrosivity of Crude Oil Feedstocks, U.S. Patent 8,956,874, February 17, 2015.

(38) Wolf, H. A.; Cao, F.; Blum, S. C.; Schilowitz, A. M.; Ling, S.; McLaughlin, J. E.; Nestic, S.; Jin, P.; Gheorghe, B. O. Method for Identifying Layers Providing Corrosion Protection in Crude Oil Fractions, U.S. Patent 9,140,640, September 22, 2015.